Structural and digestibility properties of infrared heat-moisture treated maize starch complexed with stearic acid

Clarity R. Mapengo[a], Suprakas S. Ray[a,b], M. Naushad Emmambux[a],*

[a]Department of Consumer and Food Sciences, University of Pretoria, Private Bag X20, Hatfield, Pretoria 0028, South Africa
[b]Council of Scientific and Industrial Research, National Centre of Nanostructured Material, Pretoria, South Africa

*Corresponding author. Email: naushad.emmambux@up.ac.za

Highlights

•Infrared heating can replace conventional heating for starch modification.
•Infrared HMT promotes stronger hydrogen bonds between starch molecules.
•Pasted infrared HMT starch with stearic acid had high resistant starch.
•Modified starch granules retained some of their granular structure after pasting.

Abstract

This study investigated the effects of using infrared heat-moisture treatment (IRHMT) on the properties of maize starch paste complexed with stearic acid (SA). Scanning electron micrographs showed that starch granules ghosts from IR HMT starch with SA did not show significant granular disintegration in comparison to conventionally HMT starch paste. The resistant starch (RS) content increased with SA-IR HMT, while extended pasting increased slowly digestible starch (SDS) content in IR HMT starch alone. The V polymorphs observed in XRD and DSC, and increased crystallinity from FTIR supported the changes in the properties of IRHMT starches. To a greater extent, the SA-IRHMT exerted more changes on starch micro- and molecular structural properties, and digestibility properties compared to conventional heat-moisture treatment (CHMT).

Keywords: Infrared, Heat-moisture treatment, Amylose-lipid complexes, Digestibility

1. Introduction

Starch is modified to overcome the shortcomings of native starches and diversify industrial starch application. The unbranched amylose chains have a helical conformation that can form inclusion complexes with small hydrophobic molecules such as lipids [1]. Heat-moisture treatment is widely used in starch modification. It is considered as a green chemistry method since it is a process that reduces or eliminates the use or generation of hazardous synthetic chemicals. Heat moisture treatment can change the properties of starch without destroying the starch granules [2]. Chen et al. [3] reported that HMT impacted starch granule morphology and digestibility of soy starch.

The current industrial trend is towards novel energy-efficient and environment-friendly technologies, delivering high-quality and safe processed food and food ingredients. Infrared energy can be used in food processes due to its energy & time efficiency [4]. Although much work has been conducted to investigate the starch digestibility and the structural properties of HMT starches using conventional oven heating methods, limited studies have investigated the structure and digestibility of pasted starch-lipid mixture after HMT using infrared energy.

Mapengo, Ray and Emmambux [5] worked on conventional hydrothermal treatment of maize starch with stearic acid and reported that HMT combined with stearic acid addition resulted in starch with increased resistance to acid hydrolysis. Also, in the previous work done by Mapengo and Emmambux [4], the application of infrared energy for 2 h period during HMT on maize meal influenced the structural changes that were less susceptible to enzymatic hydrolysis. However, the effect of infrared HMT may yield different results in maize starch compared to maize meal as the latter contains insignificant amounts of protein which may impact the enzymatic hydrolysis or functional properties of starch. The use of infrared energy in the HMT of maize starch could be a more convenient, less time consuming and energy-efficient way to develop starch with versatile functionality. The heating mechanism of the radiant electromagnetic energy, for example, infrared induces changes in the electronic, vibrational, and rotational states of atoms and molecules [6], promoting more amylose-amylose, amylose-amylopectin, amylopectin-amylopectin and amylose-lipid interactions within starch granules.

This current work seeks to evaluate infrared HMT's influence on the functional properties and enzymatic hydrolysis of short (10 min) and extended (120 min) pasted maize starch with SA. Therefore, the present study's overall objective was to investigate the thermal, molecular and microstructural and digestibility properties of IR HMT starch complexed with SA to produce a higher value-added starch comparable to conventional HMT starch.

2. Materials and methods

2.1. Materials

All chemicals that were used were of the highest available grade. The maize starch used had 95.8% total starch (with 24.7% amylose), 14.7% moisture, 0.6% protein, 0.3% fat, 0.06% ash content (as Dry basis except moisture). Maize starch, Glucose Assay Kit (GOPOD Format) and stearic acid were obtained from Tongaat Hulett® (South Africa), Megazyme Ltd. (Wicklow, Ireland) and Merck (Pty) Ltd. (South Africa), respectively.

2.2. Methods of preparation

2.2.1. Fatty acid addition (stearic acid/SA) and heat-moisture treatment

Stearic acid addition was done before HMT using the method by Mapengo & Emmambux [4]. Maize starch with and without stearic acid (30 g, dry basis) was weighed and put into bottles. Addition of distilled water was done while slowly stirring to adjust the moisture content to 25%. The bottles were set at 25 °C for 24 h to equilibrium moisture after which a moisture analyser was used to determine the moisture content of a homogenous sample. For conventional heat-moisture treatment (CHMT), the bottles were put in a drying oven at 110 °C for 16 h. For infrared HMT, the moisture-adjusted starch samples (30 g) were placed in an infrared oven (MW180, Olifantsfontein, South Africa) and 1000 W was applied for 1 h, 2 h and 3 h. The heat moisture treated samples were dried in a drying oven at 40 °C for 12 h. The resultant starches were cooled to room temperature and milled before analysis.

2.3. Analyses

2.3.1. Pasting and gel texture properties

A stress-controlled rheometer (Physica MC®101 model, Ostfildern, Germany) was used for pasting. A starch suspension (10% (w/w) in distilled water) was heated and cooled. The temperature was maintained at 91 °C for 10 min and 120 min corresponding to short and extended pasting, respectively. After which, the hot pastes were freeze-dried and some of the hot paste was used for gel firmness analysis. The freeze-dried starch samples were used for *in vitro* starch digestibility, scanning electron microscopy (SEM), differential scanning calorimetry (DSC), Fourier-transform infrared spectroscopy (FTIR) and X-ray diffraction scatterings (XRD) analyses. The hot paste for texture analysis was poured into plastic cylinders (diameter of 23 mm and a height of approximately 15 mm) and stored at room temperature overnight. The firmness of gels was determined with a texture analyser (EZ-L, Tokyo, Japan). A penetration test was done using a compression plate diameter of 15 mm for measuring the firmness of gel or paste.

2.3.2. *In vitro* digestion of starch

The enzymatic hydrolysis of starch was done using a method by Oladiran & Emmambux [7] with slight modifications. Starch (50 mg, dry basis) was added into a conical flask with 1 ml of boiling water before dispersed in 10 ml HCl-KCl buffer (0.2 M, pH 1.5) and 0.2 ml of pepsin enzyme solution. Starch samples were hydrolysed in a series of steps involving other enzymes outlined by Oladiran & Emmambux [7]. The hydrolysed mixtures were incubated at 60 °C for 45 min in a water bath before centrifuging the solution at 7500°×*g* for 5 min. The glucose content in the supernatant was analysed using the GOPOD assay kit. Starch fractions of RDS, SDS and RS were calculated.

2.3.3. Water solubility (WSI) and water absorption indices (WAI)

The water solubility and absorption indices of the starch samples were determined in duplicate. Distilled water (10 ml) was used to suspend the starch samples (~1 g). The starch was kept in a shaking water bath at 50 °C and 91 °C for 30 min. Sample tubes were then cooled to 25 °C. After centrifugation at 9154.3°×*g* for 15 min, the supernatant was dried at 105 °C for 16 h. The solubility (%) was calculated as the dried supernatant's weight ratio to the dry starch. The weight of the centrifuged pellet (g) per gram of the dry starch sample was the water absorption index.

2.3.4. Light microscopy (LM)

Maize starch (0.005 g, dry basis) was mixed in 1 ml of glycerol solution (30%, v/v). A small drop of the suspension was placed on a slide, and the cover was applied. The slide was observed using a Nikon Optiphot Microscope (Tokyo, Japan) under normal and polarised light.

2.3.5. Scanning electron microscopy & transmission electron microscopy

SEM was used to observe maize starch pastes' morphology using a JEOL JSM-5800 LV SEM (Tokyo, Japan) at 2500× magnification [8]. For TEM, samples were stained with osmium tetra-oxide solution. The stained samples were embedded in epoxy 812 resin before

being cut into small blocks or sections of ~100 nm. The TEM observations were made using 200 kV (accelerated voltage).

2.3.6. X-ray diffraction scatterings

The freeze-dried starch pastes were scanned by an X-ray diffractometer [X'Pert PANalytical (Eindhoven, Netherlands)] using a method by Mapengo et al. [5]. Qualitative (V polymorphs presence) and quantitative (relative crystallinity %) results were extracted from the scanned results.

2.3.7. Fourier-transform infrared spectroscopy

A Perkin Elmer Spectrum (100 FTIR spectrometer, USA) was used to scan samples from 4000 to 500 cm^{-1}. A method by Owonubi, Aderibigbe, Mukwevho, Sadiku, & Ray [9] was used for spectroscopy analysis.

2.3.8. Differential scanning calorimetry

Approximately 9 mg of the dried starch sample was weighed in a 100 µl aluminium pan. Distilled water was added for moisture content adjustments (75%, w/w wet basis), and the samples were equilibrated. The sealed aluminium pan containing the starch sample and the reference pan was heated from 25 to 140 °C at a rate of 10 °C/min. The high-pressure DSC827e (Greifensee, Switzerland) was calibrated using Indium (Tp = 156.6 °C, 28.45 Jg^{-1}).

2.4. Statistical analysis

Data were analysed by multifactor analysis of variance, LSD test using SPSS 20.0 Statistical Software Program (SPSS Incorporated, Chicago). A value of $p < 0.05$ was deemed statistically significant. Results are expressed as the average value ± standard deviation of triplicate experiments. Multivariate analysis of variance was conducted to determine the significant differences between the independent variables (SA addition, CHMT and IR HMT).

3. Results and discussion

3.1. Pasting and gel texture properties

Pasting attributes and gel firmness of native, CHMT and IR HMT starches are shown in Fig. 1 and Table 1. Significant changes were observed in pasting parameters for IR HMT starches heat- relative to non-treated samples. In both 10 min and 120 min pasting, the infrared heat-moisture treated (IR HMT) on maize starch alone and starch complexed with SA significantly ($P < 0.05$) increased the pasting temperature of the starch and decreased the peak viscosity. These results were consistent with reports in previous studies of heat-moisture treated maize starch by Sui et al. [10]. The gel firmness for IRHMT maize starch alone (after extended pasting) significantly ($P < 0.05$) increased with increase in the duration of IR exposure (1 h to 2 h). However, there was no further increase after 2 h. All pasting curves for SA-IR HMT (1 h, 2 h and 3 h) did not have distinct peak viscosity or breakdown viscosity. IRHMT significantly ($P < 0.05$) reduced the final viscosity in comparison with CHMT for pasted (10 min and 120 min) starch with SA. SA-IRHMT reduced setback viscosity and produced a non-gelling starch. The changes in pasting properties (the swelling of granules and resulted in

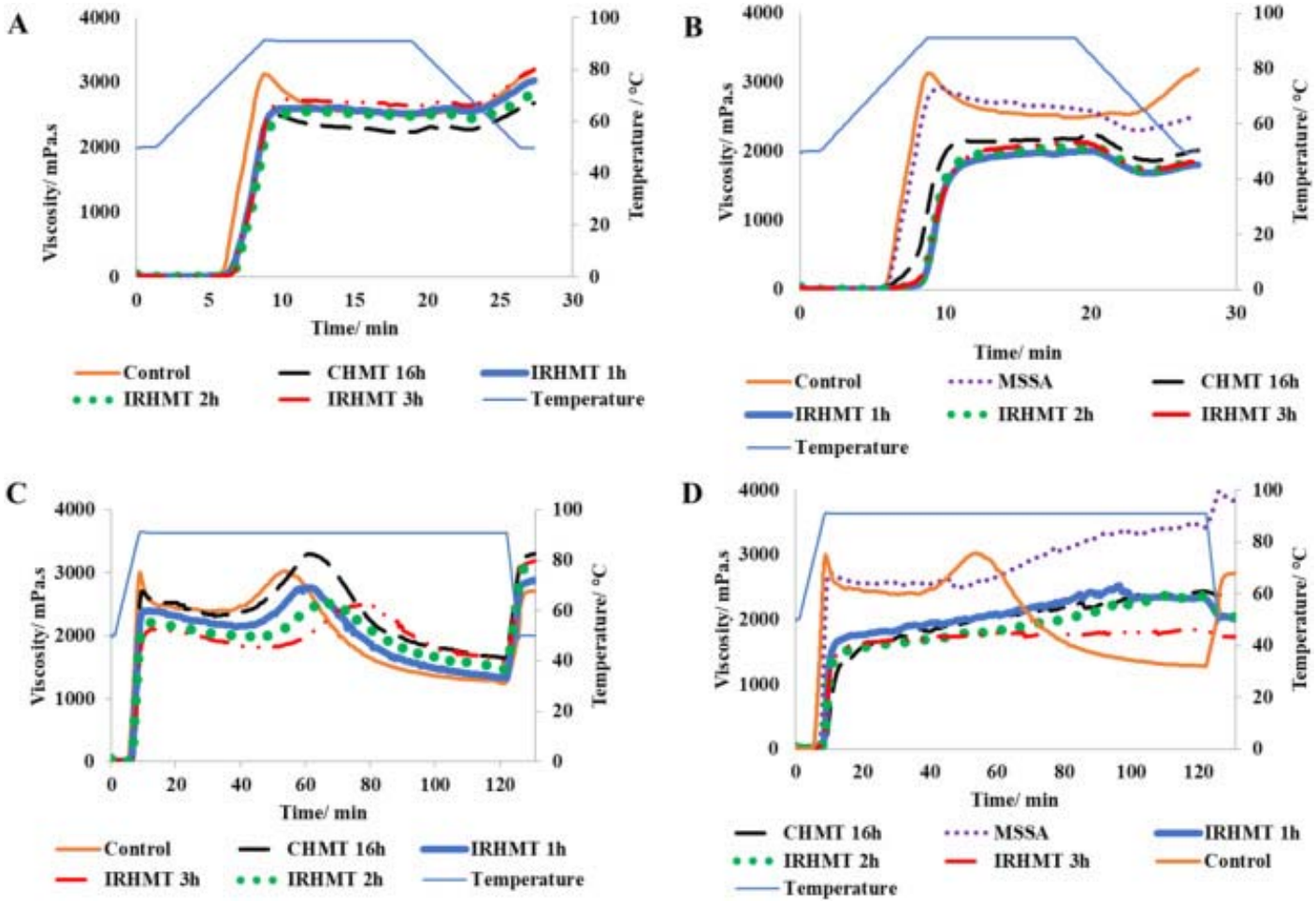

Fig. 1. The pasting profiles of CHMT and IRHMT maize starch (A- 10 min pasting maize starch & B- 10 min pasting maize starch + SA; C- 120 min pasting maize starch & D- 120 min pasting maize starch +SA; Control = native starch; MSSA = starch with SA; IRHMT 1 h = HMT using infrared energy for 1 h; CHMT = conventionally HMT for 16 h @ 110 °C; IRHMT 2 h = HMT using infrared energy for 2 h; IRHMT 3 h = HMT using infrared energy for 3 h).

Table 1. Pasting properties of CHMT and IRHMT maize starch complexed with SA.

Treatment	Short pasting			Extended pasting		
	FV (mPa·s)	SBV (mPa·s)	Gel H (N)	FV (mPa·s)	SBV (mPa·s)	Gel H (N)
None	3148d ± 41	683d ± 63	5.0b ± 0.4	2683b ± 47	634c ± 6.7	4.9c ± 0.2
Conventional HMT 16 h	2566c ± 134	360c ± 81	6.7c ± 0.3	3281c ± 30	261a ± 3.7	5.9d ± 0.1
Infrared HMT 1 h	3001d ± 41	519 cd ± 15	7.4 cd ± 0.8	2967c ± 126	295a ± 2.8	5.7d ± 0.1
Infrared HMT 2 h	2849d ± 30	368c ± 37	7.4 cd ± 0.4	3261c ± 131	389b ± 6.2	7.5e ± 0.1
Infrared HMT 3 h	2916d ± 28	412c ± 18	6.9c ± 0.6	3139c ± 71	435b ± 8.2	6.03de ± 0.1
SA	2567c ± 25	140b ± 35	1.1a ±0.2	3762c ± 72	408b ± 6.7	1.1b ± 0.1
SA + Conventional HMT 16 h	2141b ±112*	−159a ± 81*	0.5a ± 0.09*	2000ab ± 65*	−147a ± 3.6*	0.9ab ±0.1*
SA + Infrared HMT 1 h	1912a ± 144*	−194a ± 40*	0.3a ± 0.04*	2123ab ± 105*	−267a ± 2.4*	0.8a ± 0.03*
SA + Infrared HMT 2 h	1916a ± 138*	−221a ±31*	0.4a ± 0.04*	2007ab ± 41*	−315a ± 5.6*	0.7a ± 0.01*
SA + Infrared HMT 3 h	1732a ± 106*	−269a ±12*	0.3a ± 0.1*	1727a ± 15*	−136a ± 14*	0.8a ± 0.03*

A = stearic acid addition; short pasting = 10 min holding at 91 °C; extended pasting = 120 min holding at 91 °C; FV = final viscosity; SBV = setback viscosity; Gel H = gel hardness (N).

∗Statistically significant interactive effect between treatments; same letter in each column shows that the mean values are not significantly different at $P < 0.05$.

Table 2. Nutritional properties of CHMT and IRHMT maize starch complexed with SA.

Treatment	Short pasting				Extended pasting			
	RDS (%)	SDS (%)	RS (%)	eGI	RDS (%)	SDS (%)	RS (%)	eGI
None	88d ± 2.5	8a ± 0.3	4a ± 0.9	92d ± 0.4	58d ± 1.1	28b ± 0.8	14b ± 0.8	84c ± 1.3
Conventional HMT 16 h	77bc ± 2.2	13c ± 2	10bc ± 1.1	87bc ± 0.3	47c ± 0.9	43d ± 0.8	10b ± 0.8	77b ± 0.9
Infrared HMT 1 h	70b ± 1.2	18d ± 5	12c ± 3.3	86b ± 1.2	40a ± 0.9	48de ± 2.1	12b ± 0.3	74b ± 1.5
Infrared HMT 2 h	74b ± 3.7	11b ± 2.7	15c ± 3.3	84b ± 2.8	44b ± 1.7	41d ± 0.9	15bc ± 0.3	73ab ± 0.8
Infrared HMT 3 h	82c ± 1.9	11b ± 1.5	7b ± 0.4	88c ± 1	42ab ±0.7	41d ± 1.1	17c ± 0.5	74b ± 1.9
SA	71b ± 3.1	14 cd ± 5.1	14c ± 2.1	84b ± 0.9	41ab ± 1.3	44d ± 1.1	15bc ± 0.1	75b ± 4.9
SA + Conventional HMT 16 h	70b ± 2.7*	12a ± 1.7	18c ± 1.9*	79a ± 0.4*	39a ± 1.6*	43d ±0.3	18c ± 0.9*	72a ± 3.4*
SA + Infrared HMT 1 h	68a ± 1.5*	10d ± 2.3	26d ± 0.9*	76a ± 0.9*	38a ± 1.3*	39 cd ± 3	23d ± 0.4*	70a ± 1.9*
SA + Infrared HMT 2 h	64ab ±3.4*	10b ± 3.6	28d ± 1.5*	76a ± 0.6*	39a ± 0.4*	30c ± 0.6	31e ± 0.5*	70a ± 1.6*
SA + Infrared HMT 3 h	79c ± 4.8*	6a ± 2	15c ± 3.5*	84b ± 1.3	38a ± 0.9*	36c ± 1	26d ± 0.5*	70a ± 1.8*

SA = stearic acid addition; short pasting = 10 min holding at 91 °C; extended pasting = 120 min holding at 91 °C; RDS = rapidly digestible starch fraction; SDS = slowly digestible starch fraction; RS = resistant starch fraction; eGI = estimated glycaemic index.

∗Statistically significant interactive effect between treatments; same letter in each column shows that the mean values are not significantly different at $P < 0.05$.

higher pasting temperature, lower peak viscosity and reduced retrogradation) can be due to amylose-stearic acid complex formation and increased hydrogen bonding between amylopectin chains. This explanation is further discussed in details later on.

3.2. *In vitro* digestion of starch

Fig. 2 shows the hydrolysis curves for IRHMT starch alone and complexed with SA. The contents of RDS, SDS, and RS in the starch with SA during 10 min and 120 min pasting are shown in Table 2. IRHMT 1 h and IRHMT 2 h alone after short pasting had a significantly ($P < 0.05$) lower RDS and increased SDS and RS as compared to 3 h. All IRHMT maize starch alone (extended pasted) had a significantly ($P < 0.05$) higher SDS content (~48%) in comparison with other treatments (Table 2). The RS content in IRHMT maize starch with SA (short pasted) was higher than in the IRHMT maize starch without SA. IR HMT 1 h and IRHMT 2 h maize starch alone had RS content ~26% and 28% respectively, which was significantly ($P < 0.05$) higher than the CHMT maize starch with SA (~18%) (short pasted). SA-IRHMT 2 h maize starch after 10 min and 120 min pasting had the lowest estimated GI values of 76 and 70, respectively. These values were significantly lower than those of short and extended pasted SA-CHMT 16 h, which were 79 and 72, respectively.

3.3. Water solubility (WSI) and water absorption indices (WAI)

The water absorption and solubility capacity of IRHMT starch are shown in Table 3. The water absorption index and solubility index for native starch were higher ($P < 0.05$) than CHMT and IRHMT starches. The decrease in both the absorption and solubility capacity for CHMT starches was also reported by Huang et al. [11] and Olayinka, Adebowale, & Olu-Owolabi [12]. The water solubility index values (91 °C) for HMT + SA were ordered as follows: CHMT 16 h ≥ IRHMT 1 h ≥ IRHMT 2 h ≥ IRHMT 3 h. These results may support the reduced final viscosity, increased pasting time and temperature mentioned earlier (Fig. 1), suggesting that IRHMT-induced amylopectin and amylose hydrogen bonding and producing a more compact granular structure [11]. The reduction in pasting viscosity of the IRHMT starch +SA shown in Fig. 1 may have been influenced by the low water absorption capacity of starch granules restricting swelling (Table 3).

Table 3. Effects of conventional and infrared HMT on the water solubility and water absorption indices of maize starch with and without stearic acid.

Treatment	WAI 91 °C (g/g)	WSI 91 °C (%)
None	10.1e ± 0.1	2.5e ± 0.1
Conventional HMT 16 h	9.1 cd ± 0.2	2.1d ± 0.2
Infrared HMT 1 h	9.4d ± 0.1	1.9 cd ± 0.1
Infrared HMT 2 h	8.8c ± 0.2	1.7c ±0.1
Infrared HMT 3 h	9.7b ± 0.1	1.7c ± 0.1
SA	9.3d ± 0.1	1.8c ± 0.3
SA + Conventional HMT 16 h	8.5c ±0.1*	1.8c ± 0.2*
SA + Infrared HMT 1 h	7.5b ±0.2*	1.3c ± 0.4*
SA + Infrared HMT 2 h	7.3b ± 0.3*	1.2ab ± 0.1*
SA + Infrared HMT 3 h	6.8a ±0.2*	1.4a ± 0.1*

SA = stearic acid addition; WAI = water absorption index at 91 °C; WSI = water solubility index at 91 °C.

∗Statistically significant interactive effect between treatments; same letter in each column shows that the mean values are not significantly different at $P < 0.05$.

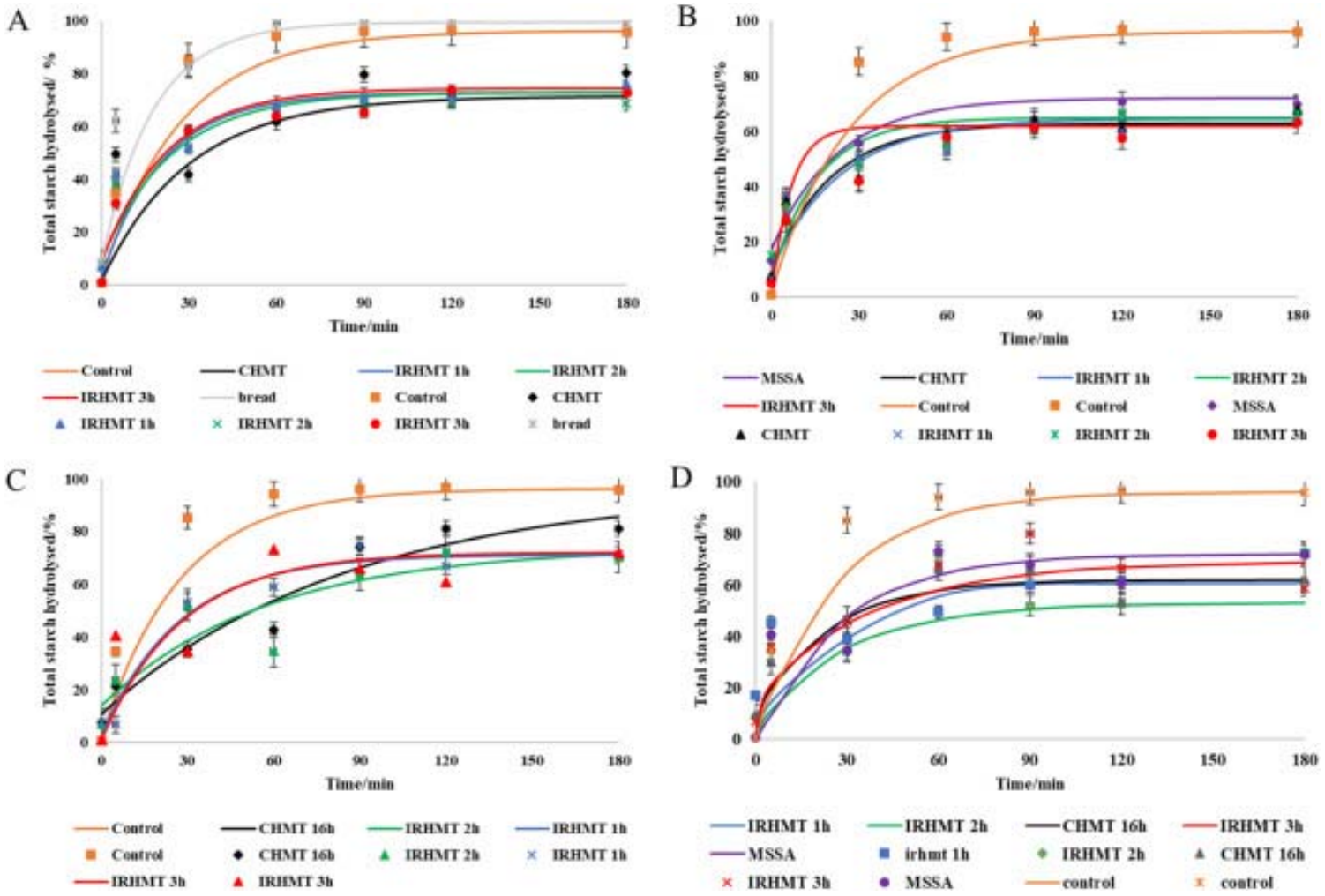

Fig. 2. *In Vitro* starch hydrolysis curves for CHMT and IRHMT maize starch pastes (A- 10 min pasted maize starch alone & B- 10 min pasted maize starch with SA; C- 120 min pasted maize starch alone & D- 120 min pasted maize starch with SA; Control = native starch; MSSA = starch with SA; IRHMT 1 h = HMT using infrared energy for 1 h; CHMT = conventionally HMT for 16 h; IRHMT 2 h = HMT using infrared energy for 2 h; IRHMT 3 h = HMT using infrared energy for 3 h).

3.4. Light microscopy (LM)

IRHMT did not seem to change the shape or size of starch granules but increased aggregates' formation (Fig. 3). The starch granule aggregation intensified by SA, and can also be attributed to SA forming a hydrophobic layer around granules. The hydrophobicity of IRHMT aggregated granules could be responsible for lower water absorption indices and lower peak viscosities values reported in Tables 3 and 1 respectively. The micrographs of IRHMT starches had clear birefringence, under polarised light suggesting that the infrared energy did not gelatinise the starch granules.

3.5. Scanning electron microscopy & transmission electron microscopy

After both 10 min and 120 min pasting, a degenerated continuous network of aggregated polymers was observed for IRHMT starch without SA in Fig. 4. This ‘net-like’ structure in the continuous phase may be consonant to the molecular entanglements of starch polymers in IRHMT starch alone. Fannon & Bemiller [13] reported similar micrographs of maize starch paste as ghost structures after cryo-preparation. The ‘ghost structures’ within the network of IR HMT maize starch were discontinuous and more substantial. This could suggest extensive starch molecules hydrogen bonding due to IRHMT. Fannon & Bemiller [13] reported similar findings on cross-linked starches. This could also indicate that IRHMT alone promoted more amylose-amylose/amylose-amylopectin/amylopectin-amylopectin interactions than the control. The extended period of pasting resulted in the network in discontinuous phase with increased thickness, volume and rigidity of ‘ghost’ microstructures in IRHMT maize starch pastes alone as compared to short pasted samples (Fig. 4).

After pasting, IRHMT starch with SA retained some of their granular structure compared to the control (Fig. 4). SA-IRHMT also retained some of their granular structure more than IRHMT starch alone. Exarhopoulos & Raphaelides [14] had similar observations on SA added to maize starch after heating at 85 °C. These observations may suggest that more amylose-fatty acid interactions took place during pasting and retarded the destruction of the granules. XRD and DSC also showed ALCs in preceding sections. The extended-pasted maize starch with HMT combined with SA showed smaller ghost structures dispersed. This could also suggest the strong association of amylose-SA and amylose-amylopectin chains resulting in low water absorption capacity (Table 3) and increased shear resistance (Fig. 1).

After pasting, the crystalline nature of the distinct nanoparticles is observed in Fig. 5. These distinct structures have been suggested to be the lamellae-like structures that aligned in the same direction in the nanoparticle. The nanomaterial could have been formed by the arrangement of crystalline regions and the presence of amylose-lipid complexes. After extended pasting and hydrolysis, Cuthbert, Ray, & Emmambux [15] observed similar structures and proposed that the distinct particles' crystalline nature could be inferred through the lamellae-like structures that aligned in the same direction in the nanoparticles (amylose-lipid complexes).

3.6. Thermal properties and crystalline structure after short pasting

Thermal properties of IRHMT starch pastes are summarised in Fig. 6. Short pasted infrared HMT maize starch alone (2 & 3 h) showed melting endotherms between 140 °C–150 °C. Retrograded amylose has a melting endotherm within a similar range [16]. After short pasting, untreated maize starch showed a weak endotherm between 97 °C–109 °C. The

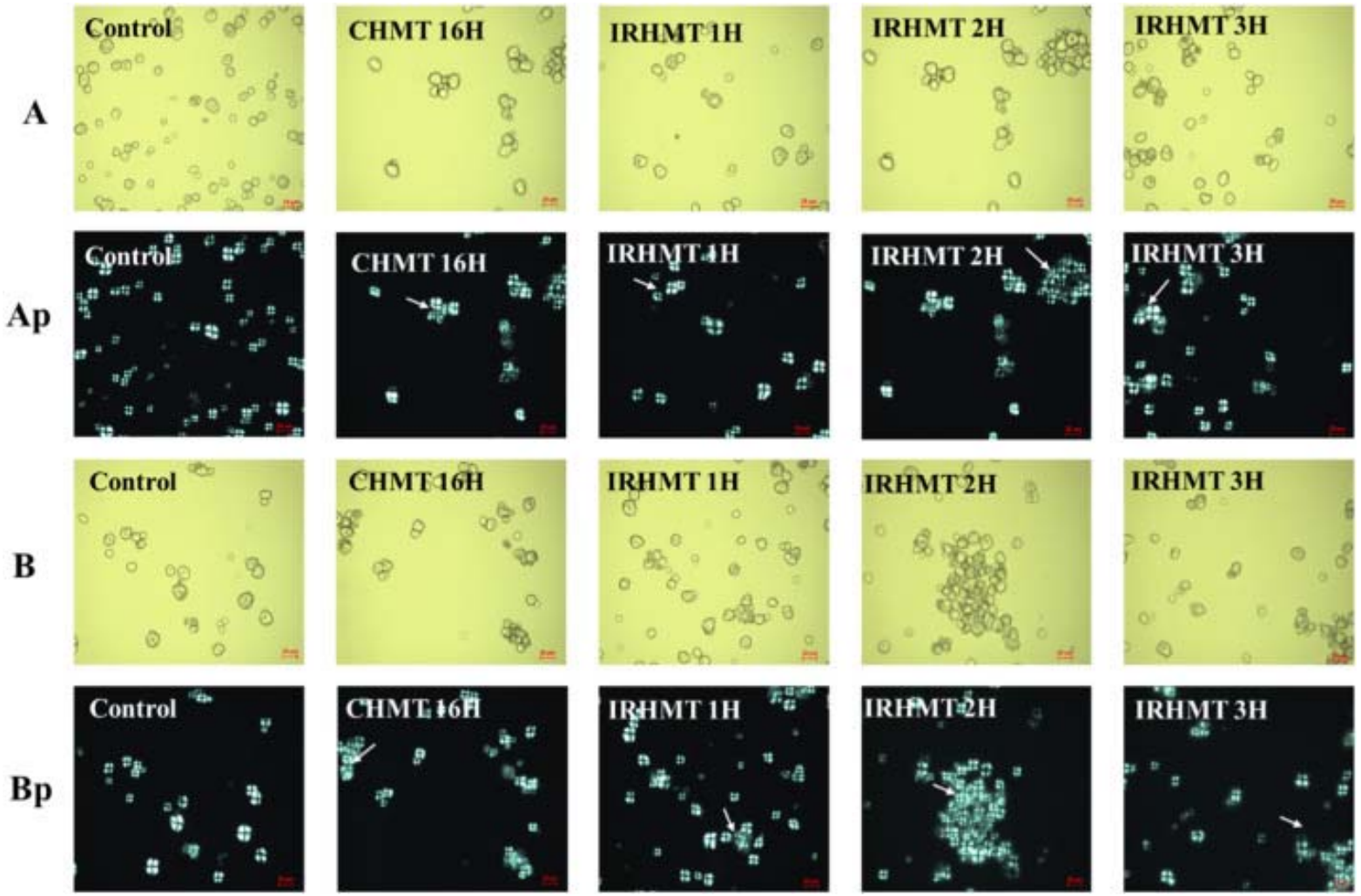

Fig. 3. Light microscopy images of HMT maize starch (Light microscopy-A &Ap represents optical light & polarised light images of starch alone respectively; B &Bp represents optical light & polarised images of starch with SA respectively).

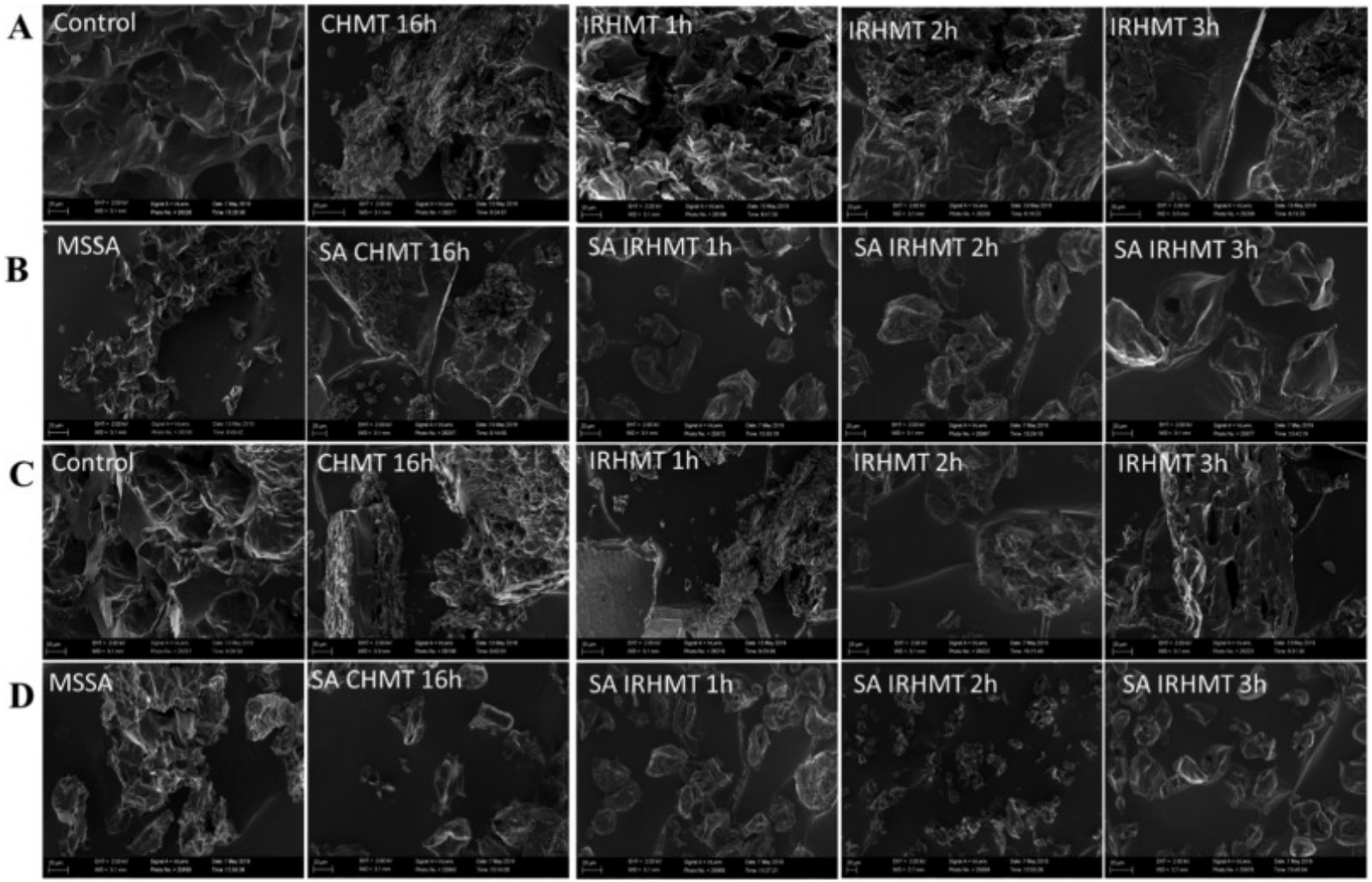

Fig. 4. Scanning electron microscopy images of HMT maize starch (-A &B represents 10 min pasted micrographs of starch alone and with SA respectively; C & D represents 120 min pasted micrographs of starch alone and with SA; control is native starch; MSSA is native starch with SA alone).

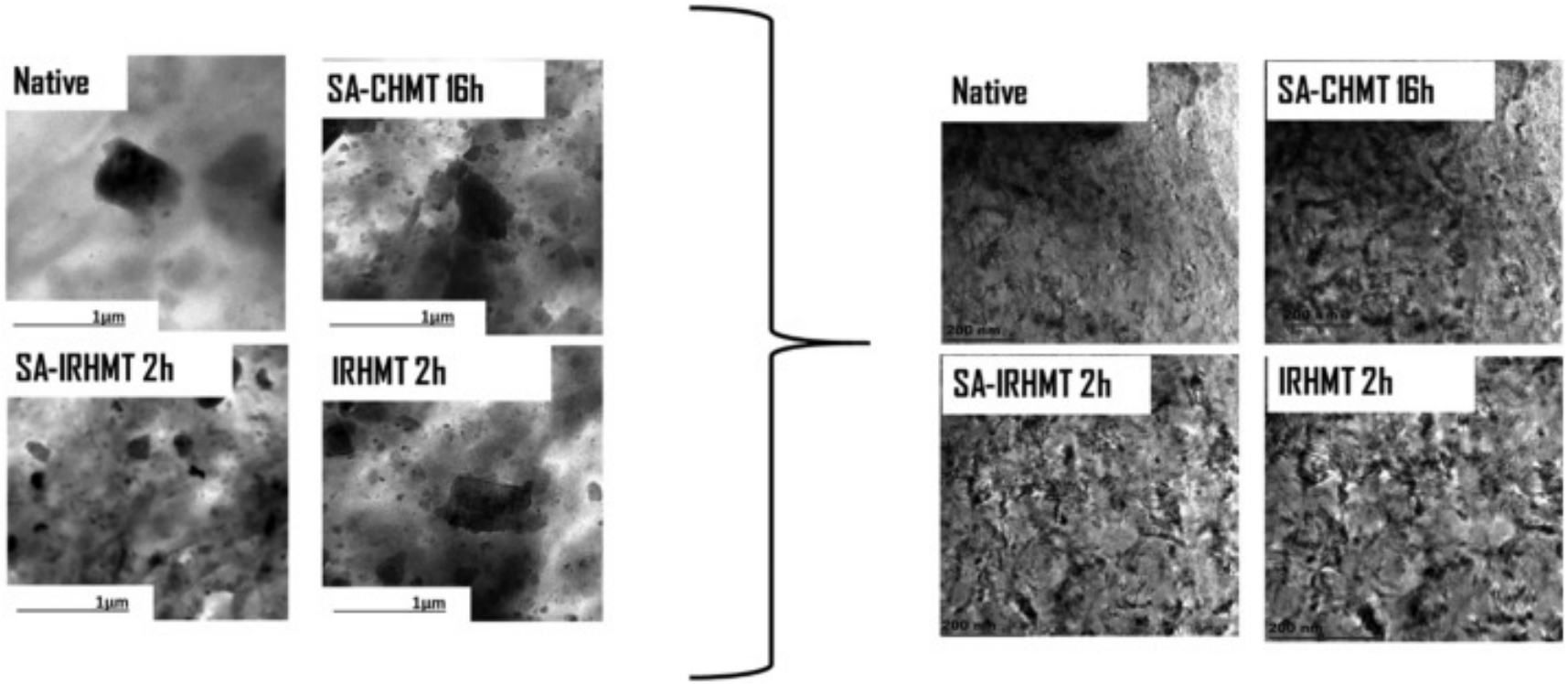

Fig. 5. Transmission electron microscopy images of HMT maize starch (native = untreated starch; SA-IRHMT 2 h = stearic acid addition + HMT using infrared energy for 2 h; CHMT = conventionally HMT for 16 h @ 110 °C; IRHMT 2 h = HMT using infrared energy for 2 h).

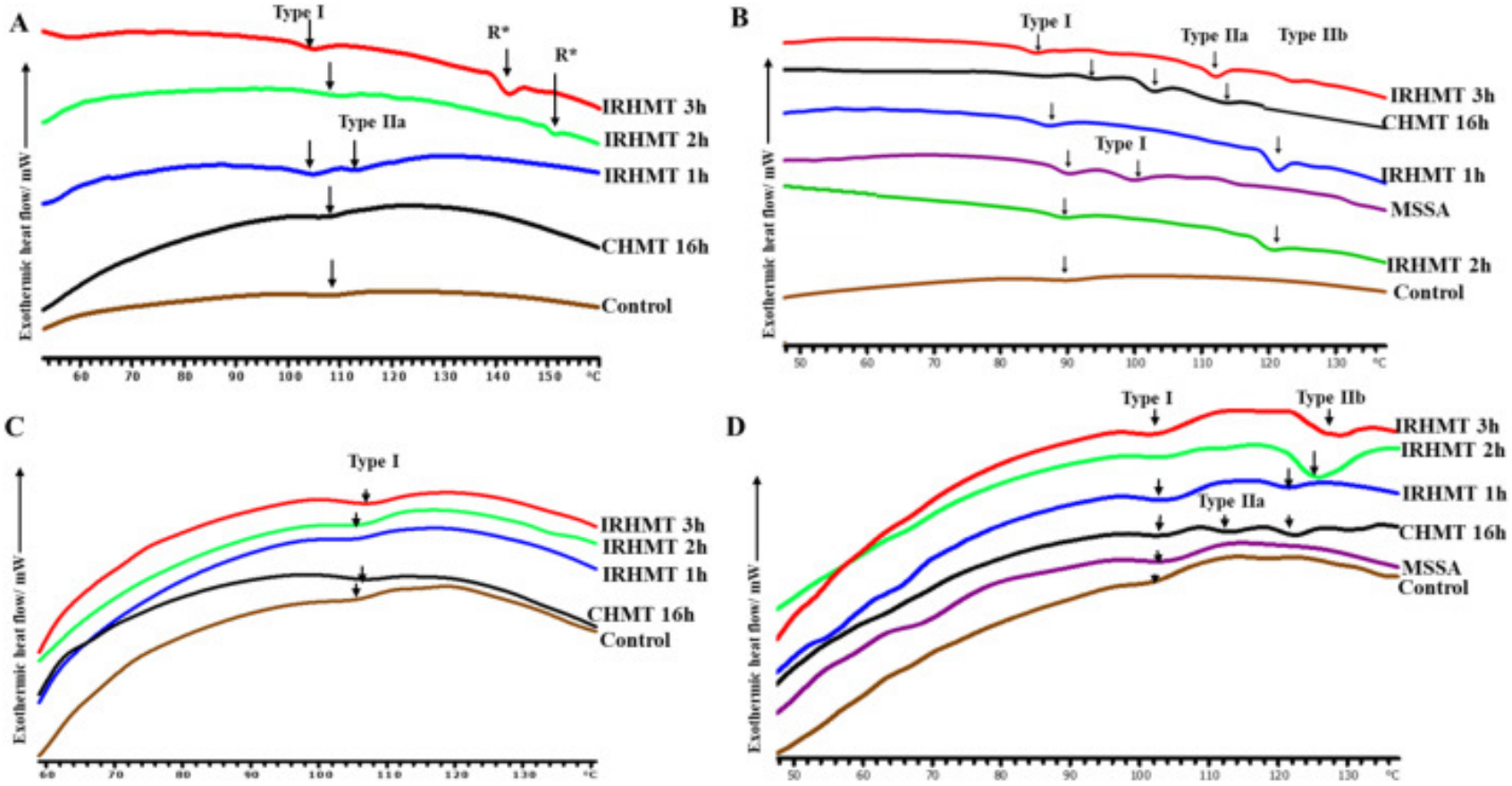

Fig. 6. DSC thermogram for CHMT and IRHMT maize starch pastes (A- 10 min pasting maize starch & B- 10 min pasting maize starch + SA; C- 120 min pasting maize starch & D- 120 min pasting maize starch +SA; Control = native starch; MSSA = starch with SA; IRHMT 1 h = HMT using infrared energy for 1 h; CHMT = conventionally HMT at 110 °C for 16 h; IRHMT 2 h = HMT using infrared energy for 2 h; IRHMT 3 h = HMT using infrared energy for 3 h).

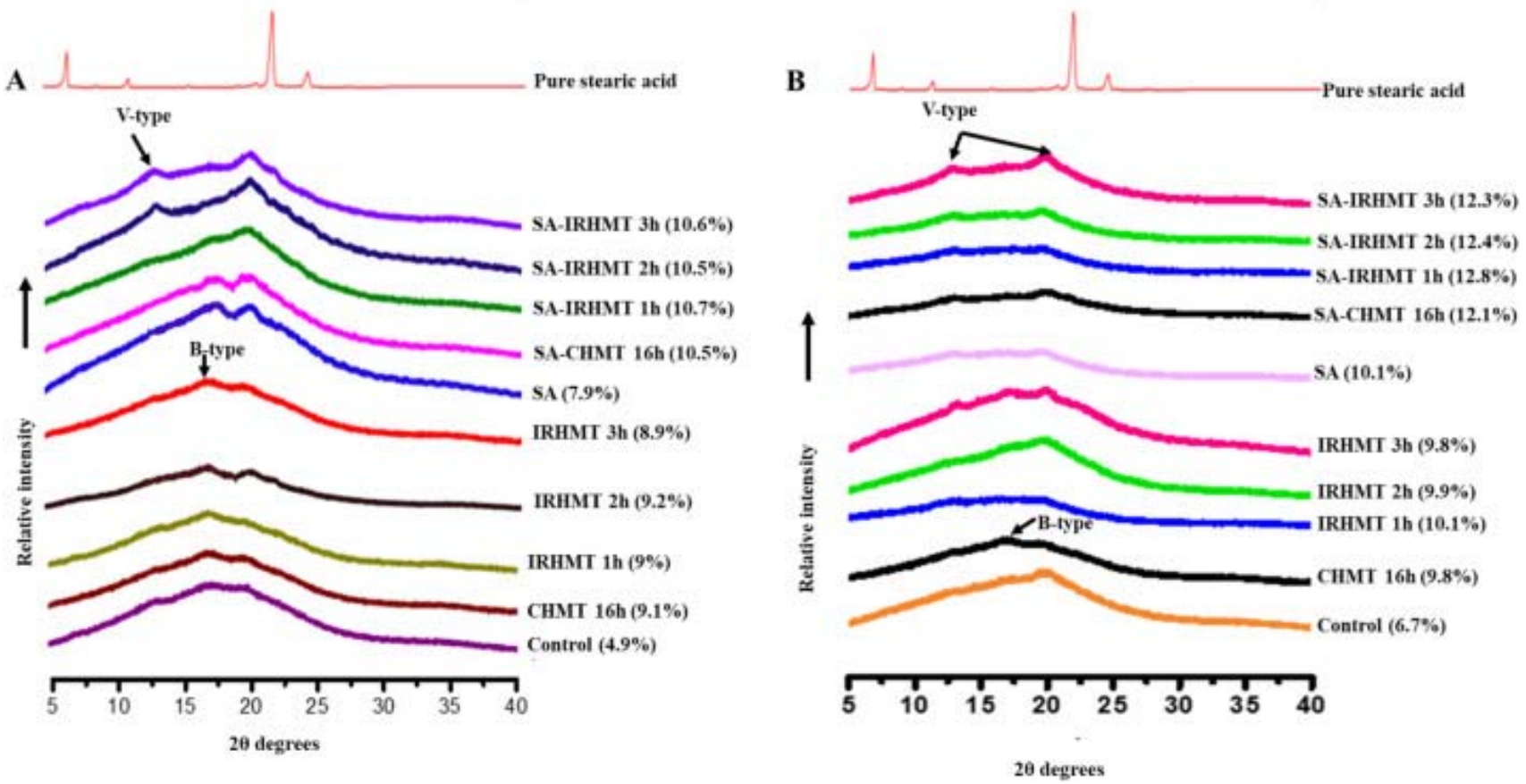

Fig. 7. XRD patterns of CHMT and IRHMT maize starch pastes (A- 10 min pasted maize starch & B- 120 min pasted maize starch; MSSA = starch with SA; IRHMT 1 h = HMT using infrared energy for 1 h; CHMT = conventionally HMT at 110 °C for 16 h; IRHMT 2 h = HMT using infrared energy for 2 h; IRHMT 3 h = HMT using infrared energy for 3 h).

melting endotherms with a melting temperature between 94 °C and 104 °C and between 115 °C and 121 °C correspond to type I and type II amylose-lipid complexes (ALCs) respectively to the type I amylose-lipid complexes. After short pasting, native starch showed a peak around 2θ = 17° and a weak peak around 2θ = 13° (Fig. 7A). Maize starch with SA alone had two peaks at 2θ = 17° and 2θ = 20°. The peaks around 2θ = 13° and 2θ = 20° correspond V-type crystalline structure (ALCs). The retrograded crystallites confirmed by XRD peak at 17 for IRHMT maize starch support the retrograded starch melting endotherms reported in Fig. 6A for IRHMT maize starch after short pasting. The relative crystallinity values for the native starch without & with SA were 4.9% and 7.9%, respectively.

IRHMT maize starch without SA (after short pasting) showed an endotherm corresponding to type I ALCs (Fig. 6A). There was no significant ($P > 0.05$) difference in the enthalpy for the endotherm observed for all HMT maize starch alone (Supplementary Table 1). All IRHMT maize starch samples without SA showed a distinct XRD peak at 17° and a weak peak around 20°. The peak around 20° corresponds to V complexes and support the type I ALCs endotherms observed in Fig. 6A. These ALCs are due to the amylose bonding with naturally occurring lipids. The distinct peak at 17° corresponding to retrograded starch as mentioned earlier suggests that IRHMT promoted more amylose-amylose, amylose-amylopectin and amylopectin-amylopectin reassociation [5]. The increase in more hydrogen bonding is more evident in the high relative crystallinity values for IRHMT starches, which were significantly ($P < 0.05$) higher than native starch. The increased crystallinity due to retrograded starch crystallites is consistent with slowly digestible starch for CHMT and IRHMT starches alone (Table 2). The high values for crystallinity were also supported by the high 1047/1022 cm^{-1} band ratio for IRHMT maize starch in Fig. 8. A higher ration of the 1047/1022 cm^{-1} corresponds with increased relative crystallinity [17]. The FTIR spectra also show that IRHMT starch paste (2 h) had more distinct peaks around ~858, 762 and 708 cm^{-1} (Fig. 8). The peaks at 861 cm^{-1} and 764 cm^{-1} have been ascribed to COH bending and CH_2-related modes. These bands are sensitive to changes in starch molecular structure [18].

Multiple endotherms were observed for SA-CHMT and SA-IRHMT (after short pasting) (Fig. 6B). These endotherms corresponded with type I, IIa and type IIb amylose-lipid complexes. IRHMT maize starch with SA (2 h) had a more defined endotherm between 120 and 130 °C with a significantly ($P < 0.05$) higher enthalpy of ~1.3 J/g in comparison to the one for CHMT maize starch alone. Type IIa and type IIb ALCs indicate transformation to larger and more stable crystallites [19]. The presence of more stable type IIb ALCs in IRHMT combined with SA (2 h) could explain the increased RS reported in Table 2, as ALC can be resistant to alpha-amylase hydrolysis [4]. The formation of the amylose−SA complexes and more ordered crystallites was consistent with the restricted swelling of starch granules (Table 3) and the reduced starch hydrolysis shown in Fig. 2.

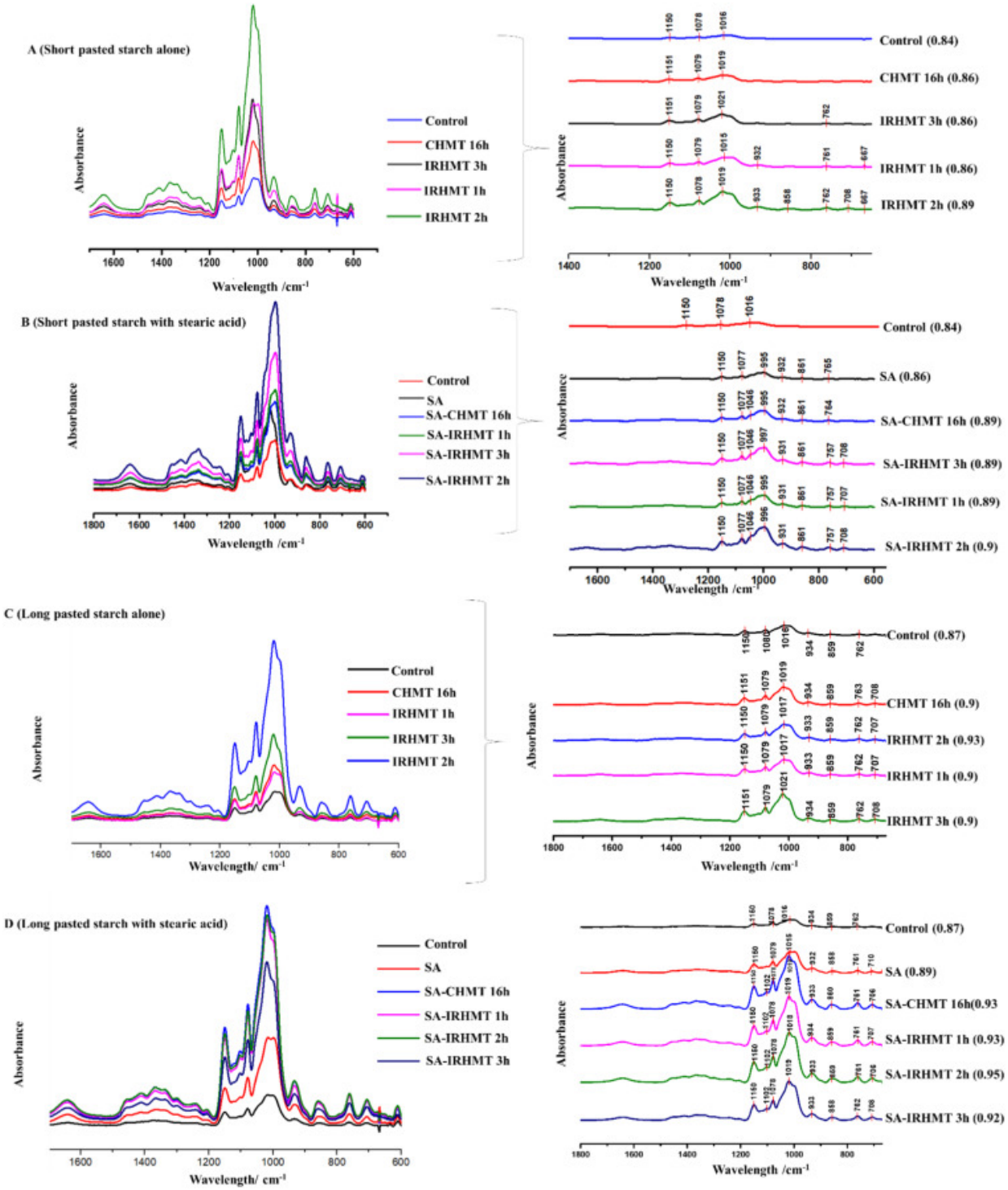

Fig. 8. FTIR spectra of HMT maize starch pastes (A & B- 10 min pasted maize starch alone and with SA respectively; C & D- 120 min pasted maize starch alone and with SA respectively; Control = native starch; MSSA = starch with SA; IRHMT 1 h = HMT using infrared energy for 1 h; CHMT = conventionally HMT at 110 °C for 16 h; IRHMT 2 h = HMT using infrared energy for 2 h; IRHMT 3 h = HMT using infrared energy for 3 h).

X-ray diffraction patterns for CHMT starch with SA exhibited peaks at both 17° and 20° while IRHMT 2 h and IRHMT 3 h on maize starch with SA resulted in XRD peak at 13° and

20°. The absence of a peak at 17° could suggest that IR heating promoted more amylose-SA interaction rather than more amylose-amylose/amylose-amylopectin/amylopectin-amylopectin reassociation (retrograded starch) in IRHMT starch (2 h & 3 h). The % crystallinity of SA-IRHMT starches was higher than that of maize starch without SA. These results were further supported by the FTIR spectra, which showed that SA + IRHMT maize starch had a higher value for the ratio of 1047/1022 cm^{-1} suggesting increased starch polymer hydrogen bonding in the amorphous region.

The absorbance band of FTIR at 995 cm^{-1} (Fig. 8) is related to the water–starch interaction, and its absorption intensity is produced by the C–O–H bending vibrations, and 1047 cm^{-1} correspond to crystalline structures in starch [17]. IRHMT samples showed the high intensity of the peak at ~1710 cm^{-1} which corresponds to the vibration of the carbonyl group of stearic acid. The 1047/1022 cm^{-1} band ratio of on SA-IRHMT was higher than that of IRHMT alone (Fig. 8). Kawai et al. [20] reported a reduced susceptibility to hydrolysis for gelatinised potato starch–fatty acid mixtures and attributed this decrease to the interactions between starch and fatty acids, which are more resistant to alpha-amylase digestion.

3.7. Thermal properties and crystalline structure after extended pasting

After extended pasting, HMT samples had one distinct endotherm between 98 and 110 °C (Fig. 6C). The enthalpy for native maize starch endotherm was ~0.2 J/g. The enthalpy for this endotherm for IRHMT starch alone was significantly ($P < 0.05$) higher than that of short pasted maize starch samples. More heat-stable complexes of type II could be present during prolonged heat treatment [21]. IRHMT (2 & 3 h) had a significantly ($P < 0.05$) higher enthalpy for amylose-lipid complexes around ~0.6 J/g in comparison with CHMT (~0.4 J/g).

After extended pasting, native maize starch had relative crystallinity of ~6.9%, and maize starch with SA had a relative crystallinity of ~10.1% (Fig. 7B). All infrared HMT samples alone had an XRD peak around ~7° and 17° (Fig. 7B). V_h-type amylose has major peaks at diffraction angles 2θ of about 7.3°, 12.9°, 19.8° [22]. IRHMT promoted amylose-lipid complex formation with endogenous lipids hence the peak at ~7°. These findings are also supported by the FTIR spectra (Fig. 8) showing distinct peaks with increased intensity around 752 and 708 cm^{-1}. The peak at 17° was more distinct in extended pasted IRHMT maize starches without SA in comparison with the IRHMT starches after short pasting (Fig. 7A). This suggests that prolonged pasting of IRHMT starches promoted more amylose-amylose/amylose-amylopectin & amylopectin-amylopectin reassociations which explains the increased gel strength of infrared HMT starches after extended pasting as compared to after short pasting (Table 1). The ratio of 1047/1022 cm^{-1} for IRHMT starch alone after 120 min pasting was higher than that of 10 min pasted starches. The CHMT starch alone, IRHMT starch for 1 h, 2 h and 3 h had a relative crystallinity of about 9.8%, 10.1%, 9.9% and 9.8% respectively as shown by XRD in Fig. 7.

CHMT maize starch with SA had three endotherms corresponding to type I, type IIa and type IIb ALCs with an enthalpy of 0.37 J/g, 0.44 J/g and 1.1 J/g respectively. All IRHMT starch samples (1, 2 & 3 h) with SA had two endotherms corresponding to type I and type IIb ALCs with an enthalpy of ~0.64 J/g and ~1.5 J/g respectively. It has been suggested that infrared energy promotes the interaction of amylose–lipid helices to facilitate nucleation of type IIa to form type IIb during pasting. The melting temperature of the type IIb ALCs for IRHMT maize starch with SA was significantly ($P < 0.05$) higher than all other treated samples (~135 °C).

All extended-pasted maize starch with SA showed two XRD peaks around 13° and 20°. IRHMT starch with SA had higher intensities for the XRD peaks observed (Fig. 7B). These peaks suggest that HMT resulted in more amylose-SA complexes rather than the formation of B-type crystallites (retrograded starch). The DSC has also shown the presence of ALCs melting endotherms in HMT starch with SA (Fig. 6D). The CHMT starch with SA, IRHMT starch with SA for 1 h, 2 h and 3 h had a relative crystallinity of about 12.1%, 12.8%, 13.1% and 12.9% respectively. The increased relative crystallinity for IRHMT maize starch with SA suggests improved starch chain and SA interactions during HMT resulting in more stable crystallites after pasting. DSC confirmed that these crystallites as type IIb ALCs with a very high enthalpy (Fig. 6D and Supplementary Table 1). The FTIR peaks at 1150, 1102, 1079, 858, 762 and 708 cm^{-1} for IRHMT starch with SA were narrower, with a higher amplitude for SA-IRHMT. The ratio of 1047/1022 cm^{-1} for SA-IRHMT was greater than that of native starch (Fig. 8).

Overall SA coupled with IRHMT increased the relative crystallinity of starch due to the formation of new crystallites (hence the increased 1047/1022 cm^{-1} band ratio), which corresponds with the increased resistance to enzymatic hydrolysis discussed earlier. Mapengo et al. suggested that more ordered crystalline regions in conventionally HMT starch with SA hide the α1–4 glycosidic bonds, thereby making modified starch less susceptible to acid hydrolysis. Since the results of SA-IRHMT are comparable to those of conventional HMT, the overall findings of this paper could also suggest that IRHMT can produce starch applicable in the production of low pH foods as highlighted by the conventional HMT results from the previous work [5].

Overall, in the presence of stearic acid, both extended and short pasting promoted more amylose-stearic acid interaction and less amylose-amylose interactions in infrared HMT starch with stearic acid thereby enhancing the possibility of complex restoration or new complex formation (Fig. 9). The ALCs conformation has been reported to inhibit enzyme-substrate formation, thereby making the starch less digestible [20]. ALCs inhibit the enzyme-substrate interaction, and this seems to support the role of ALCs in reduced starch digestibility highlighted in the model. In support of this model, Mapengo and Emmambux [4], also indicated that the increase in the RS content as a result of increased interactions between amylose and amylopectin.

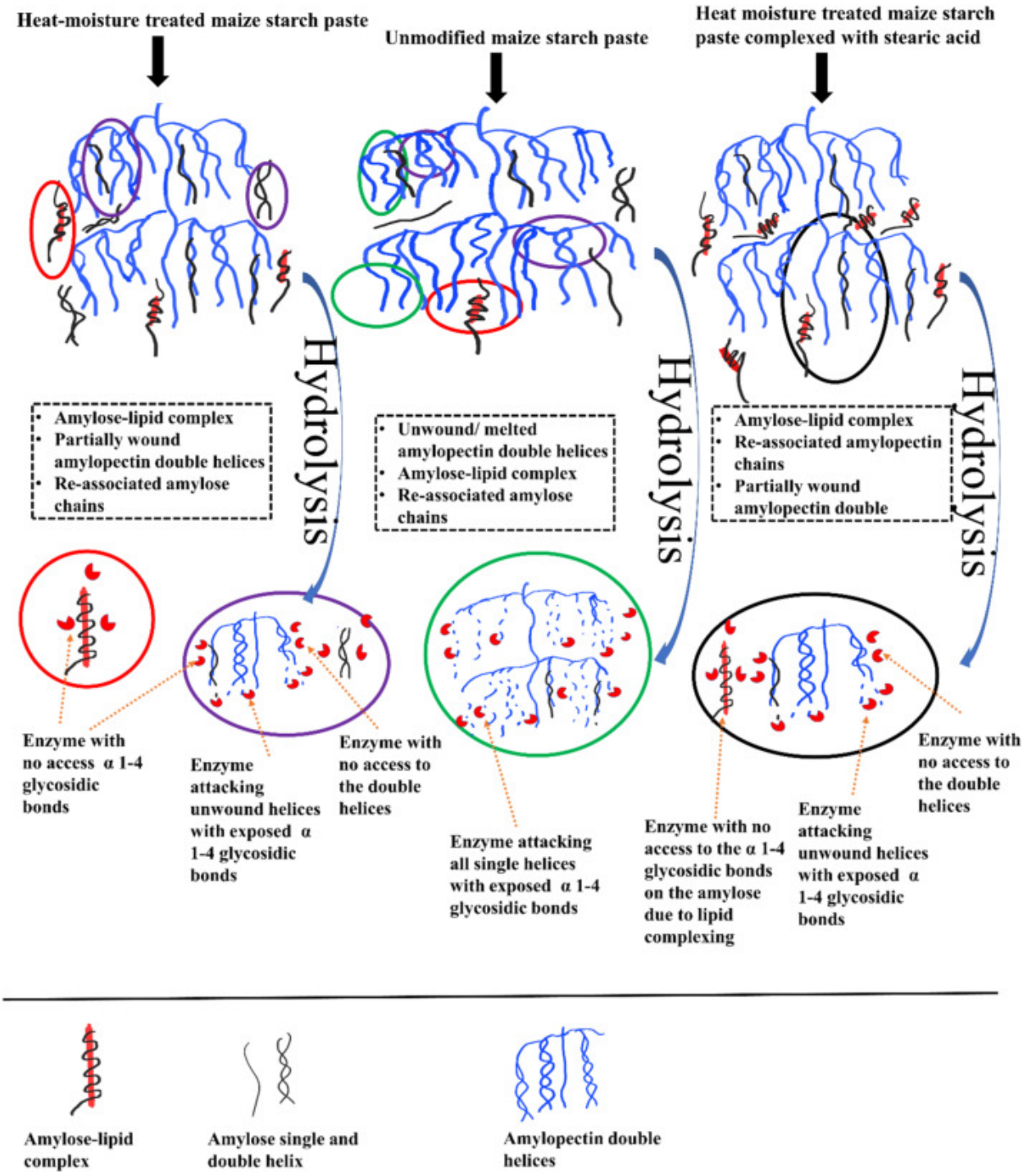

Fig. 9. Schematic diagram illustrating how heat moisture treatment and stearic acid addition facilitates structural changes that enhance the functional properties of starch.

4. Conclusions

Infrared energy increases the mobility of amylose and amylopectin and promotes more hydrogen bonding and amylose-amylose reassociations. This increased hydrogen bonding promotes gel strength and an increase in slowly digestible starch for infrared heat moisture

treated maize starch alone. A combination of infrared energy and stearic acid addition promotes the formation of more amylose-SA complexes to form a non-gelling starch and a further reduction in the estimated glycaemic index through the formation of resistant and slowly digestible starch. The ALCs block junction zones' formation to inhibit retrogradation in infrared heat moisture treated maize starch with stearic acid. Therefore, infrared HMT can produce versatile starches with potential use as functional ingredients in the food industry.

CRediT authorship contribution statement

Suprakas Sinha Ray: Funding acquisition, Supervision. **Mohammad Naushad Emmambux**: Project administration, Funding acquisition, Supervision; Conceptualization, Reviewing and Editing, Validation. **Clarity Ropafadzo Mapengo**: Methodology, Software, Formal analysis, Investigation, Writing- Original draft preparation and Visualization.

Hypothesis statement

The use of infrared energy during HMT may influence the structural changes in starch granules and result in the formation of new starch crystallites that are less susceptible to enzymatic hydrolysis.

Declaration of competing interest

All authors declare that there is no conflict of interest related to this article.

Acknowledgements

The authors would like to acknowledge the University of Pretoria, Council of Scientific and Industrial Research of South Africa and the DSI/NRF Centre of Excellence in Food Security for support and funding from grant ID 91490.

References

References
[1] J. Putseys, L. Lamberts, J. Delcour, Amylose-inclusion complexes: formation, identity and physico-chemical properties, *J. Cereal Sci*. 51 (3) (2010) 238–247.
[2] A.O. Ashogbon, E.T. Akintayo, Recent trend in the physical and chemical modification of starches from different botanical sources: a review, *Starch-Stärke* 66 (1–2) (2014) 41–57.
[3] X. Chen, J. Luo, L. Fu, D. Cai, X. Lu, Z. Liang, L. Li, Structural, physicochemical, and digestibility properties of starch-soybean peptide complex subjected to heat moisture treatment, *Food Chem.* 297 (2019), 124957, https://doi.org/10.1016/j.foodchem.2019.124957.
[4] C.R. Mapengo, M. Naushad Emmambux, Functional properties of heat-moisture treated maize meal with added stearic acid by infrared energy, *Food Chem.* 126846 (2020)https://doi.org/10.1016/j.foodchem.2020.126846.
[5] C.R. Mapengo, S.S. Ray, M.N. Emmambux, Pasting properties of hydrothermally treated maize starch with added stearic acid, Food Chem. 289 (2019) 396–403, https://doi.org/10.1016/j.foodchem.2019.02.130.
[6] C. Skjöldebrand, *Infrared heating, Thermal Technologies in Food Processing*, Elsevier 2001, pp. 208–228.

[7] D.A. Oladiran, N.M. Emmambux, Nutritional and functional properties of extruded cassava-soy composite with grape pomace, *Starch - Stärke* 70 (7–8) (2018) https://doi.org/10.1002/star.201700298.
[8] T. Liu, Y. Ma, S. Xue, J. Shi, Modifications of structure and physicochemical properties of maize starch by γ-irradiation treatments, *LWT Food Sci. Technol*. 46 (1) (2012) 156–163.
[9] S. Owonubi, B. Aderibigbe, E. Mukwevho, E. Sadiku, S.S. Ray, Characterization and in vitro release kinetics of antimalarials from whey protein-based hydrogel biocomposites, *Int. J. Ind. Chem*. 9 (1) (2018) 39–52.
[10] Z. Sui, T. Yao, Y. Zhao, X. Ye, X. Kong, L. Ai, Effects of heat-moisture treatment reaction conditions on the physicochemical and structural properties of maize starch: moisture and length of heating, *Food Chem*. 173 (2015) 1125–1132, https://doi.org/10.1016/j.foodchem.2014.11.021.
[11] T.-T. Huang, D.-N. Zhou, Z.-Y. Jin, X.-M. Xu, H.-Q. Chen, Effect of repeated heat-moisture treatments on digestibility, physicochemical and structural properties of sweet potato starch, *Food Hydrocoll*. 54 (2016) 202–210.
[12] O.O. Olayinka, K.O. Adebowale, B.I. Olu-Owolabi, Effect of heat-moisture treatment on physicochemical properties of white sorghum starch, *Food Hydrocoll*. 22 (2) (2008) 225–230.
[13] J.E. Fannon, J.N. Bemiller, Scanning electron microscopy after cryopreparation, *Cereal Chem*. 69 (4) (1992) 456–460.
[14] S. Exarhopoulos, S.N. Raphaelides, Morphological and structural studies of thermally treated starch-fatty acid systems, *J. Cereal Sci*. 55 (2) (2012) 139–152.
[15] W.O. Cuthbert, S.S. Ray, N.M. Emmambux, Isolation and characterisation of nanoparticles from tef and maize starch modified with stearic acid, *Carbohydr. Polym*. 168 (2017) 86–93, https://doi.org/10.1016/j.carbpol.2017.03.067.
[16] R. Eerlingen, Formation, Structure and Properties of Enzyme Resistant Starch, 1995.
[17] P. Martínez, F. Peña, L.A. Bello-Pérez, C. Núñez-Santiago, H. Yee-Madeira, C. Velezmoro, Physicochemical, functional and morphological characterization of starches isolated from three native potatoes of the Andean region, *Food Chem.: X* 2 (2019), 100030, https://doi.org/10.1016/j.fochx.2019.100030.
[18] J.D. Hoyos-Leyva, L. Alonso-Gomez, J. Rueda-Enciso, H. Yee-Madeira, L.A. Bello-Perez, J. Alvarez-Ramirez, Morphological, physicochemical and functional characteristics of starch from *Marantha ruiziana Koern, LWT Food Sci. Technol*. 83 (2017) 150–156, https://doi.org/10.1016/j.lwt.2017.05.019.
[19] G. Rappenecker, P. Zugenmaier, Detailed refinement of the crystal structure of Vh-amylose, *Carbohydr. Res*. 89 (1) (1981) 11–19.
[20] K. Kawai, S. Takato, T. Sasaki, K. Kajiwara, Complex formation, thermal properties, and in-vitro digestibility of gelatinized potato starch–fatty acid mixtures, *Food Hydrocoll*. 27 (1) (2012) 228–234.
[21] F. Tufvesson, M. Wahlgren, A.C. Eliasson, Formation of amylose-lipid complexes and effects of temperature treatment. Part 2. Fatty acids, *Starch-Stärke* 55 (3–4) (2003) 138–149.
[22] G. Gelders, T. Vanderstukken, H. Goesaert, J. Delcour, Amylose–lipid complexation: a new fractionation method, *Carbohydr. Polym*. 56 (4) (2004) 447–458